Volume 22, No 4 | International Journal of Radiation Research, October 2024

Impact of neoadjuvant chemotherapy and cytoreductive surgery on patients with advanced ovarian cancer based on bioinformatics analysis

L. Luo, W. He, Q. Guo, CY. Wang*

Department of Gynaecology, Affiliated Hospital of Southwest Medical University, Sichuan Provincial Center for Gynaecology & Breast Disease, China

► ***Original article***

***Corresponding author:**
Chunyan Wang, Ph.D.,
E-mail:
wangchunyan0215@126.com

Received: January 2023
Final revised: February 2024
Accepted: February 2024

Int. J. Radiat. Res., October 2024; 22(4): 1009-1017

DOI: 10.61186/ijrr.22.4.1009

Keywords: *Ovarian cancer, neoadjuvant chemotherapy, cytoreductive surgery, differentially expressed genes, tertiary lymphoid structure, immune infiltration.*

ABSTRACT

Background*:** surgery (CRS) and neoadjuvant chemotherapy (NACT) are recommended for advanced ovarian cancer (aOC) treatment. This study aimed to investigate the therapy-induced genomic changes and immune microenvironment alteration in patients with aOC. ***Materials and methods: The microarray data of ovarian cancer samples from naïve or treated patients were collected from the Gene Expression Omnibus (GEO) database, and the differentially expressed genes (DEGs) between samples were screened. Consensus clustering was conducted to explore the molecular subtypes of ovarian cancer samples. The correlation between tertiary lymphoid structure (TLS) signatures with the molecular subtypes was subject to Gene set variation analysis (GSVA). The prognostic signature of aOC was constructed using machine learning based on lasso-cox regression. Finally, immune infiltration analysis was performed for immune landscape evaluation in aOC. ***Results:*** Totally 28 DEGs were found between the control and treatment groups. Enrichment analysis indicated the association of these genes with the immune changes. Moreover, the cluster 1/2 (C1/C2) of ovarian cancer were identified, and the C1 subtype had higher enrichment of TLS-related biomarkers. Moreover, 15 genes were revealed as independent factors for the prediction of ovarian cancer prognosis. Immune infiltration levels were significantly higher in the C1 subtype, which indicated the distinct immune landscape between the two molecular subtypes of ovarian cancer. ***Conclusion:*** The NACT and CRS induced genomic changes were related to immune response in aOC. The findings of our study might deepen our understanding of the TLS-related signature and immune pattern in aOC patients.

INTRODUCTION

Ovarian cancer is a lethal gynaecological cancer with nearly 314, 000 new cases and over 207, 000 death cases globally in 2020 [1]. The cytoreductive surgery (CRS) followed by neoadjuvant chemotherapy (NACT) is recommended as the front-line standard of care for ovarian cancer. Unfortunately, due to the late diagnosis at advanced stage, most patients recur after a median of 10 to 18 months, and the 5-year survival rate is about 45% [2,3]. NACT combined with CRS is considered as an opportunity for advanced ovarian cancer (aOC) patients not suitable for primary cytoreductive surgery in recent years [4,5], with improved outcomes and reduced postoperative mortality [6]. Currently, the large genomic studies of ovarian cancer such as The Cancer Genome Atlas (TCGA) mainly focus on the treatment-naïve patients, which hinders the exploration of the impact of therapy on ovarian cancer. The investigation of the genomic effects of treatment remains an unmet need to predict the treatment response and efficacy in aOC patients.

Cancer is increasingly recognized as an evolutionary and ecological process with dynamic and mutual interactions related to tumor cells as well as tumor microenvironment (TME) [7,8]. TME comprises different types of cells such as fibroblasts and immune cells and extracellular components. TME controls tumor initiation, development as well as metastasis and significantly affects the treatment efficacy, and thus attracting increasing attention in the targeted cancer therapy [7,9]. Studies on TME have revealed that the anti-tumor immune response occurs in not only secondary lymphoid organs (SLOs) but also the tertiary lymphoid structures (TLSs) resembling SLOs. They are present in nonlymphoid tissues at locations of persistent inflammation such as malignancies [10]. They are indicated to promote the aggregation of immune cells to the tumor site, thus the development of TLSs is associated with the survival of treatment-naïve cancer patients [11]. Moreover, studies have also revealed that the TLS development is also correlated with the improved immunotherapy response in cancer patients receiving immune checkpoint inhibitors, suggesting

[DOI: 10.61186/ijrr.22.4.109]

the critical role of TLSs in improving anti-tumor immunity and therapeutic response [12,13]. Additionally, in ovarian cancer, studies have revealed that the TLS coordinates the infiltration of T cells as well as antibody-producing plasma cells to enhance the anti-tumor response [14,15]. However, the association between TLSs and the effects of neoadjuvant chemotherapy in ovarian cancer demands further exploration.

TLSs with prognostic and predictive value have attracted increasing attention in cancer therapy. Multiple works have described the gene signature landscape of TLSs in different cancers. For example, a study has concluded the gene signatures for TLSs in human cancers and indicates that the induction of TLSs may contribute to the anti-cancer therapy [16]. Lu *et al*. have reported that the TLS signature showed prognostic value in ovarian cancer [17]. Therefore, it is imperative to explore the impact of treatment on TLSs in advanced ovarian cancer for the prediction of treatment response and efficacy.

The present work aimed to explore the neoadjuvant chemotherapy and cytoreductive surgery induced genomic changes in ovarian cancer patients at advanced stage based on the expression data from the GEO database. The DEGs between the control and treated patients were screened and subject to enrichment analysis. The molecular subtypes of ovarian cancer patients were identified based on consensus clustering, and the correlation between the TLS signature with the subtypes was analyzed by GSVA. Machine learning was applied to construct the prognostic model in ovarian cancer based on the lasso-cox regression model. The immune cell infiltration in ovarian cancer subtypes was also analyzed. The results of our work might deepen our understanding of the treatment induced genomic changes related to immune response and provide novel prognostic biomarkers for aOC patients.

MATERIALS AND METHODS

Data collection, pre-processing and screening of differentially expressed genes

The microarray datasets of ovarian cancer (GSE14764, GSE17260) from the GEO database (http://www.ncbi.nlm.nih.gov/geo) were retrieved. GSE14764 contained 80 ovarian carcinoma samples from the GPL96 platform, and GSE17260 had 110 ovarian cancer samples from aOC patients receiving cytoreductive surgery and a platinum/taxane-based chemotherapy from the GPL6480 platform. The two datasets were merged by the inSilicoMerging R software [18], and then the batch effects were removed using the methods by Johnson WE *et al*. [19]. Finally, the data matrix with removing the batch effects was obtained. The DEGs between the treatment and control group in ovarian cancer patients were selected with limma R package under |log2 fold change(FC)| >1, adjusted P less than 0.05 and visualized with "Pheatmap" R package. Gene ontology (GO) and kyoto encyclopedia of genes and genomes pathway (KEGG) enrichment analyses for DEGs were conducted combined with the condition of |logFC| > 0.5, adjusted P < 0.05 via the R package "clusterProfiler" and "ggplot2" was applied for calculating Z score and visualization of enriched GO terms and KEGG pathways in bar plots.

Consensus clustering and identification of the TLS characteristics

The molecular subtypes of ovarian cancer cases were determined using the "ConcensusClusterPlus" R package. For the determination of optimal cluster number, the cumulative distribution function (CDF) plot was adopted, with clustering variable k from 2 to 10. The consensus clustering was conducted with K-means algorithm upon 1-pearson correlation distances. Subsequently, the optimum cluster numbers were identified and the procedures were repeated 1000 times for the stability and reproducibility of the results. The pheatmap function was used for the creation of a cluster map in R software.

Then we explored the TLS characteristics in different ovarian cancer subtypes. Totally 38 TLS-related markers were retrieved based on a previous study [16]. Gene expression pattern was obtained from GEO database, with gene annotation files (V22, V23) in human beings in gff format downloading from the GENCODE (https://www.gencodegenes.org/human/). The mapping information of GeneSymbol and ENSG_ID was retrieved and the ENSG_ID was mapped to the GeneSymbol. Finally, the expression profile after ID conversion was obtained. The GSVA was carried out to analyze the correlation between TLS characteristics and different ovarian cancer subtypes. The differential expression analysis of TLS-related genes between the subtypes were conducted with the limma package.

Identification of DEGs in subtypes and enrichment analysis of the DEGs

DEGs in ovarian cancer subtypes were screened with the independent samples t-test under the condition of |log2FC| > 1, adjusted P < 0.05. The GO as well as KEGG enrichment analyses as well as Gene Set Enrichment Analysis (GSEA) of the DEGs was performed with the "clusterProfiler" R package, and the "GOplot" package was adopted for result visualization.

Development of prognostic signature in ovarian cancer

Least absolute shrinkage and selection operator

[DOI: 10.61186/ijrr.22.4.109]

(LASSO) is an algorithm of machine learning based on regression. It is used to punish over-fitting based on logistic regression [20]. The data of survival time, event and gene expression in ovarian cancer patients were collected and combined, and the LASSO-Cox regression model was generated with the glmnet R software with 5 fold cross-validation for the establishment of the optimal model. Multivariate Cox regression was conducted for the construction of a prognostic signature based on the selected genes.

Immune infiltration analysis

Microenvironment Cell Populations-counter (MCPcounter) algorithm was used to compare the infiltration of stromal and immune cells in the C1 and C2 subtypes [21], and results were output with "Pheatmap" R package. ESTIMATE algorithm was adopted for the calculation of the stromal and immune scores for the assessment of immune infiltration in the samples of the C1 and C2 subtypes using the ESTIMATE" R package. The single-sample genomic enrichment analysis (ssGSEA) algorithm was also applied to assess the infiltrating levels of immune cells in the C1 and c2 subtypes with the GSVA R package. Cibersort software was adopted for analyzing the infiltration ratio of 12 immune cell types in C1/C2 subtype in tumor tissues based on the immune cell proportion. The statistical difference of immune infiltration levels was subject to the Wilcox-on test.

Statistical analysis

R software (version: 4.2.1) was applied for data analysis and visualization. P value < 0.05 indicated statistical significance. The differential expression in ovarian cancer subtypes was analyzed with the independent samples t-test, and differential immune infiltration levels between subtypes were analyzed with Wilcoxon test.

RESULTS

Identification of the differentially expressed genes in aOC patients after treatment

Two GEO datasets (GSE14764, GSE17260) retrieved from the GEO database were merged. As shown in the box plots figure 1A, the upper panel showed that sample distribution across the two datasets were largely different before batch-removing. However, after removing the batch effects, the medians of samples were in line and the distribution of samples was aligned (low panel, figure 1A). Similarly, the density and UMAP diagrams also revealed that the batch effects were removed in the merged datasets (figure 1B-C). Then we explored the DEGs in the tumor samples from control or treated patients under the condition of |log2FC| > 1 and adjusted P < 0.05. Totally 28 DEGs were found, 18 upregulated RNAs and 10 downregulated RNAs included, as exhibited in the heatmap (figure 1D). Moreover, we also conducted the GO and KEGG enrichment analyses for the DEGs with the condition of |logFC| > 0.5. GO analysis depicted the enrichment of these DEGs in actin filament network formation, positive regulation of leukocyte tethering or rolling, cardiac neural crest cell migration involved in outflow tract morphogenesis and cardiocyte differentiation in biology process (BP), lipoprotein particle receptor activity, oligosaccharide binding, low-density lipoprotein particle receptor activity and carboxylic acid binding in molecular function (MF). In terms of KEGG analysis, these genes were mainly enriched in the signalings related to allograft rejection, African trypanosomiasis, Asthma and Cell adhesion molecules, suggesting the involvement of the DEGs in the immune system or immune disease-related pathways.

Consensus clustering and the TLS characteristics of ovarian cancer subtypes

On the basis of consensus clustering, the RNA expression pattern after removing batch effects were classified into different subtypes. According to the CDF curves and area under the curves, we found that K = 2 was the optimal choice (figure 2A-B). Moreover, the samples were distinctly divided into two subtypes when k=2 as shown in the tracking plot (figure 2C). The consensus values were high (> 0.8) for all subtypes only in the K = 2 classification (figure 2D). These ovarian cancer samples were thus classified to the C1 (n = 60) or C2 subtypes (n = 49) (figure 2E). Next, we explored the TLS characteristics between the two subtypes based on GSVA enrichment analysis. The results indicated that the C1 subtype presented higher TLS score than C2, which indicated that C1 subtype was closely correlated with the TLS characteristics (Figure 2F). Moreover, most TLS-related RNAs were differentially expressed in the two subtypes, which demonstrated that most TLS-related transcripts were highly expressed in the C1 subtype (figure 2G).

Identification of DEGs between ovarian cancer subtypes and related pathways

We then investigated the DEGs between two molecular subtypes in ovarian cancer. The results showed that among the totally 620 DEGs, 164 RNAs were up-regulated and 456 RNAs were down-regulated (figure 3A-B). Then the GO and KEGG enrichment analysis was conducted for these genes, respectively. The bubble chart depicted that main enrichment of the down-regulated RNAs in the biological activities of immune cells as well as immune responses, for example, these genes were enriched in positive regulation of leukocyte and lymphocyte activation in biological process, collagen-containing ECM, and immunoglobulin complex in cellular component and antigen binding, structural constituent of extracellular matrix (ECM)

[DOI: 10.61186/ijrr.22.4.109]

and immunoglobin receptor binding in molecular function. KEGG analysis demonstrated the enrichment of down-regulated genes in the cytokine-cytokine receptor interaction and chemokine signalings (figure 3C). The bar plot revealed the primary enrichment of the up-related RNAs in the biological activities related to cilium structure and functions and signaling pathways associated with metabolism (figure 3D). Furthermore, the GO, KEGG combined with fold change (FC) analyses indicated that the DEGs were mainly linked with immune response, biological activity of immune cells, extracellular matrix and chemokine related pathways (figure 3E-G). Then GSEA was conducted and revealed that the DEGs were mainly associated with the immunoregulation of interactions between immune cells, scavenging of Heme from plasma, fcgamma receptor fcgr dependent phagocytosis, fceri mediated Nf-Kb activation, parasite infection, and role of phospholipids in phagocytosis (figure 3H).

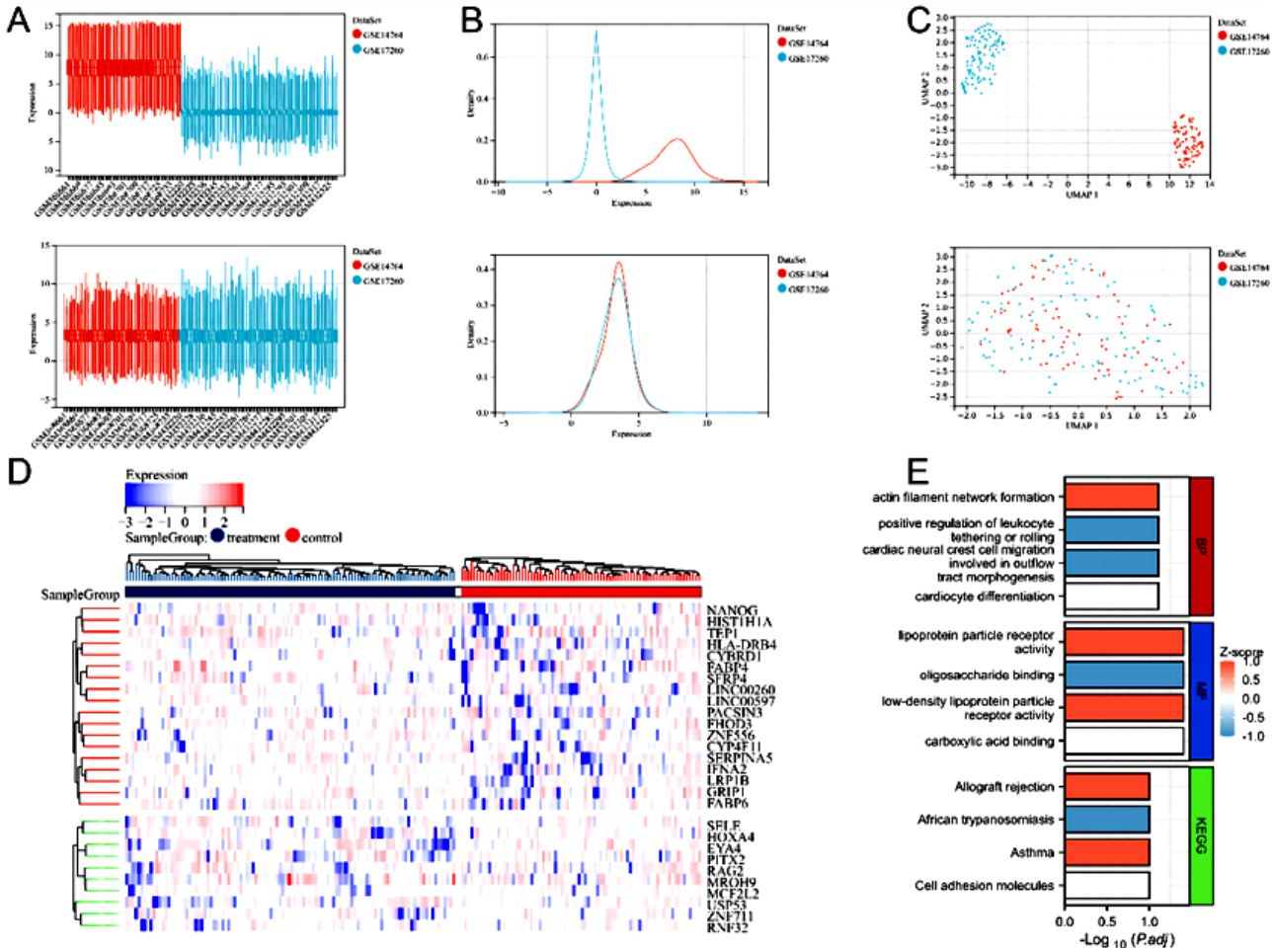

Figure 1. Data processing and screening of differentially expressed genes in treatment-naïve or treated advanced-stage ovarian cancer patients. The GEO datasets (GSE14764, GSE17260) were merged and **(A)** box plot, **(B)** density and **(C)** UMAP diagrams showed the sample distribution before (upper panel) and after (lower panel) removing batch. **(D)** The heatmap of the DEGs in control ovarian cancer patients and patients receiving cytoreductive surgery and neoadjuvant chemotherapy. Red indicated the up-regulated genes and green represented the down-regulated genes. **(E)** Bar plot of the GO and KEGG analysis for DEGs.

[DOI: 10.61186/ijrr.22.4.109]

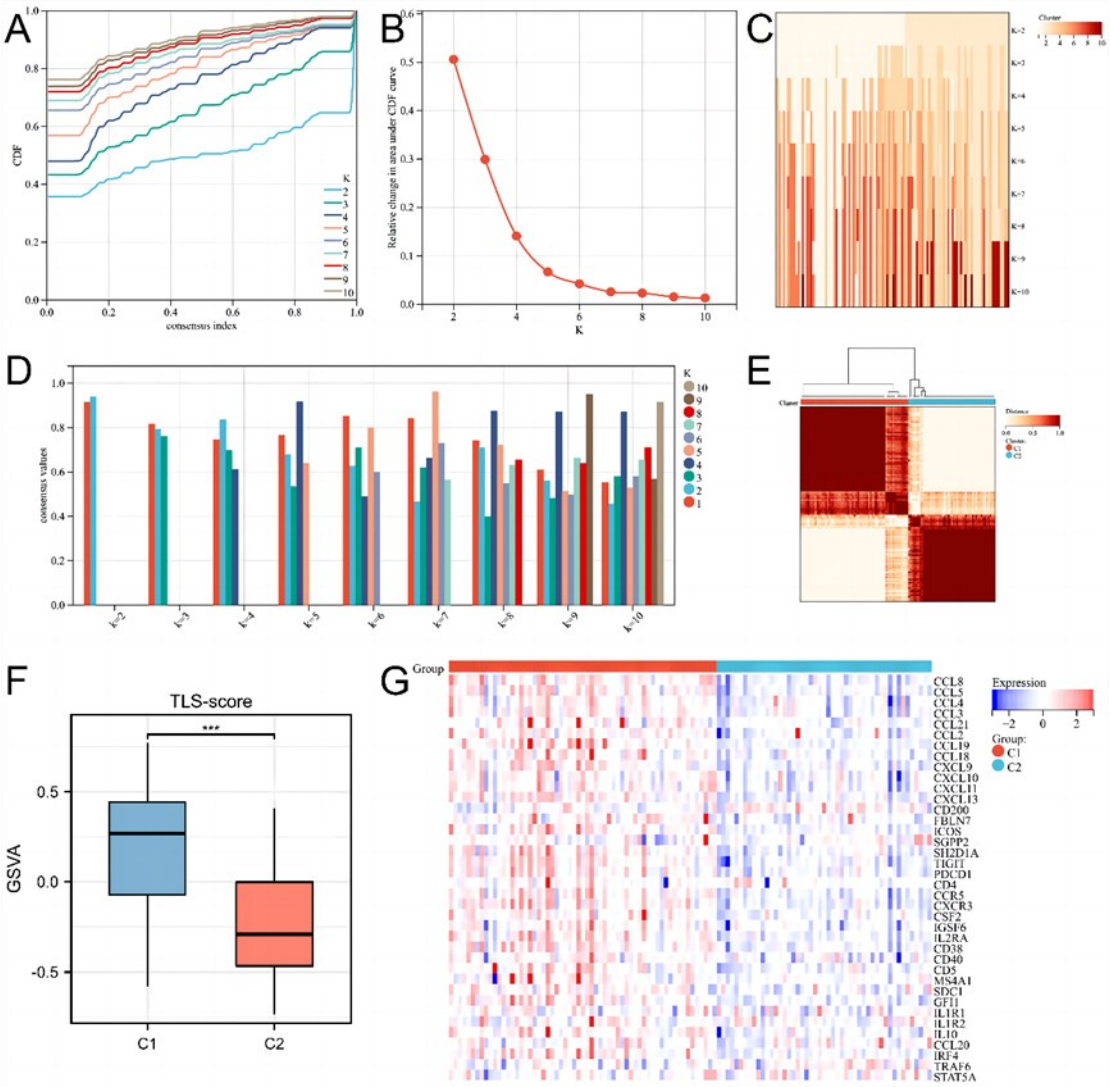

Figure 2. Identification of molecular subtypes of ovarian cancer and related TLS signature in different subtypes based on consensus clustering. **(A)** CDF curves and **(B)** area under the curves between K=2 and K=10. **(C)** Tracking plot and **(D)** Bar plot of consensus values showed the clustering consistency among samples. **(E)** Heatmap of consensus clustering of the two subtypes. **(F)** Box plot of the correlation between TLS signature and C1/C2 subtypes based on GSVA. **(G)** Heatmap showed the differential expression of TLS-related genes between the C1 and C2 subtypes.

[DOI: 10.61186/ijrr.22.4.109]

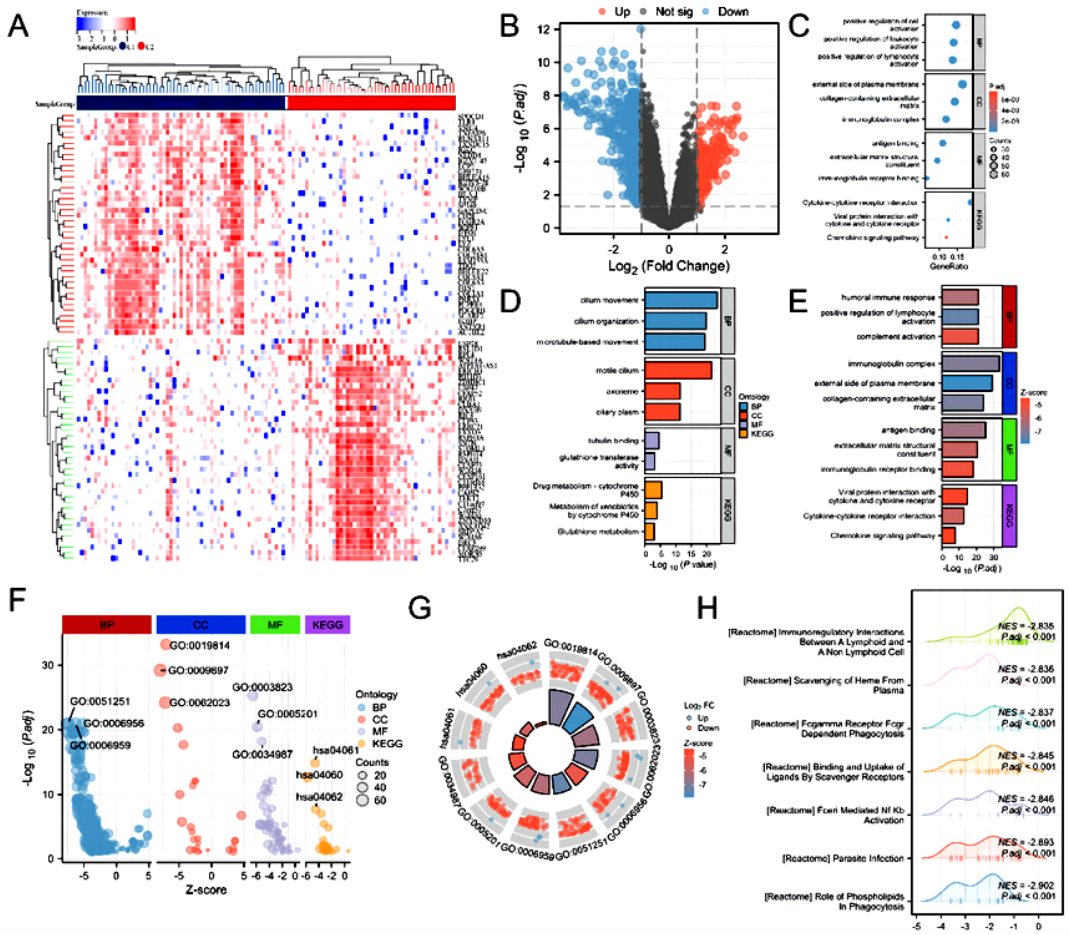

Figure 3. Identification and enrichment analysis of different expressed genes in the two molecular subtypes of ovarian cancer. **(A)** The top 40 up-regulated genes and down-regulated genes between the C1 and C2 subtypes were presented in the heatmap. **(B)** The volcano plot of the DEGs in the two subtypes. The results of GO and KEGG analysis of the **(C)** down-regulated genes and **(D)** up-regulated genes. The results of GO and KEGG analysis combined with the FC were shown in **(E)** bar chart, **(F)** GO bubble plot and **(G)** GO Circle diagram. **(H)** The Gene Set Enrichment Analysis (GSEA) of the DEGs between two molecular subtypes in ovarian cancer.

Construction of the prognostic model based on machine learning

To select the prognostic genes in ovarian cancer, Lasso-cox regression was conducted and the optimal Lambda was 0.11 after five cross-validations. Finally, a set of 31 genes were identified. (figure 4A-B). Then value of the 31 signature genes in predicting the prognosis of the 110 cases was evaluated, and the multivariate analysis showed that 15 genes were identified for constructing a predictive model for the prognosis prediction in ovarian cancer. The difference in prognostic significance was logtest = 1.33383785261384e-11, sctest = 1.46078821354154e-09, waldtest = 0.00149642809217795, C-index = 1. Totally seven genes were identified as risk factors with HR > 1, and eight genes were considered to be protective factors with HR < 1 in ovarian cancer (figure 4C).

Immune infiltration analysis

The immune cell abundance in the C1 and C2 subtypes was further evaluated. According to MCP-counter analysis, the immune cells including T cells, lymphocytes, B lineage, Natural killer (NK) cells, monocytic lineage, myeloid dendritic cells, neutrophils, endothelial cells as well as fibroblasts were mainly enriched in the C1 subtypes of patients (figure 5A). Moreover, the ESTIMATE analysis evaluated the immune and stromal scores in the C1/C2 subtypes. The results showed that patients in C1 had significantly elevated stromal and immune infiltrating levels relative to C2 (figure 5B). According to ssGSEA analysis, the infiltration proportion of immune cells in C1 and C2 subtypes of ovarian cancer patients was assessed. The levels of infiltrating immune cells such as activated or immature dendritic cells (aDCs, iDCs), B cells, Cytotoxic cells, macrophages, neutrophils, NK cells and T cells were significantly higher ($P < 0.05$) in the C1 subtype relative to the C2 subtype (figure 5C-D). Furthermore, Cibersort analysis revealed that the naïve B cells, memory resting CD4 T cells, regulatory T cells and monocytes were mainly infiltrated into the tissues of C2 subtypes (figure 5E). Overall, these results indicated that C1 molecular subtype had enhanced anti-tumor immune defense compared with the C2 subtype.

[DOI: 10.61186/ijrr.22.4.109]

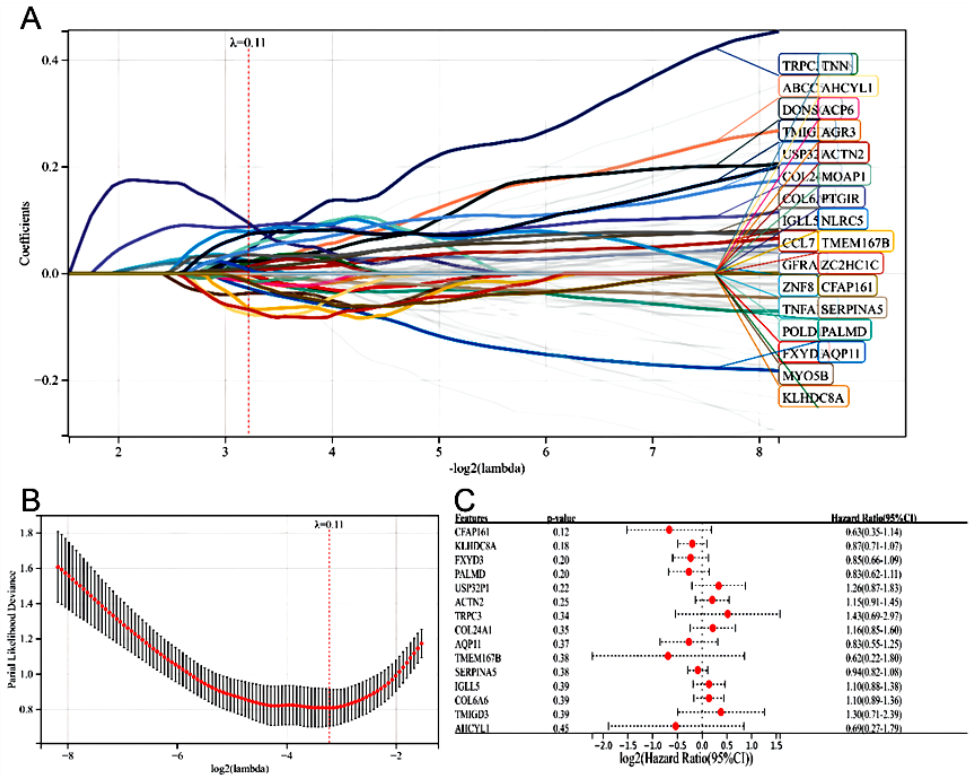

Figure 4. Construction of the prognostic signature based on Lasso-Cox regression in ovarian cancer. **(A-B)** The Lasso-Cox regression coefficients for the selected genes. **(C)** multivariate analysis was performed to identify the independent prognostic factors.

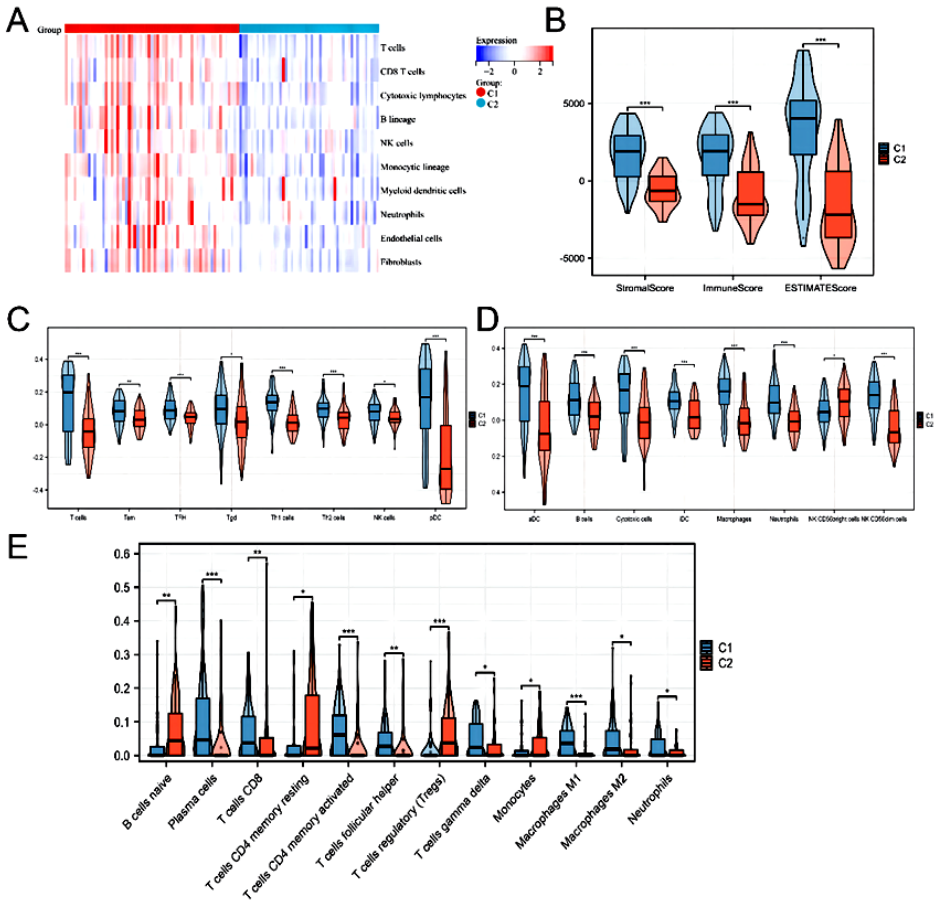

Figure 5. Immune Infiltration status in the molecular subtypes of ovarian cancer. **(A)** The heatmap of MCPcounter analysis showed the abundance of immune cells in the C1 and C2 subtypes. **(B)** The Estimate analysis revealed the Stromal Score, Immune score and ESIMATE score of the C1 and C2 subtypes. **(C-D)** The ssGSEA and **(E)** Cibersort analysis showed the abundance of different types of immune cells in the C1 and C2 subtypes.

[DOI: 10.61186/ijrr.22.4.109]

DISCUSSION

Ovarian cancer as the most fatal gynecologic tumor is often diagnosed at the advanced stage. The cytoreductive surgery and neoadjuvant chemotherapy is recommended to improve the prognosis in ovarian cancer patients at late stage [22]. Exploration of genomic signature in response to surgery and chemotherapy contributes to the design of the adaptive treatment strategies [23]. In our work, we explored the DEGs between naïve aOC patients and aOC patients receiving cytoreductive surgery and neoadjuvant chemotherapy. The ovarian cancer patients were divided into two molecular subtypes and C1 subtype was closely related to TLS gene signature. Then the DEGs between the subtypes were screened and enrichment analyses revealed that these DEGs were associated with immune response and biological activities of immune cells. The prognostic model was constructed based on Lasso-Cox regression, and the independent prognostic factors for ovarian cancer were identified. Furthermore, we also discovered that the C1 subtype showed elevated immune infiltration levels into tumors.

In this study, two GEO datasets (GSE14764, GSE17260) with naïve or treated advanced ovarian cancer patient samples were merged and the batch effects were removed. Totally 28 DEGs between the control and treated aOC patients were selected, 18 upregulated and 10 downregulated genes included. Then GO and KEGG analysis was conducted combined with the fold change analysis, revealing that the DEGs in treated ovarian cancer patients were mainly related to the immune system and immune response, suggesting the treatment-induced immune changes in advanced ovarian cancer patients (figure 1). Furthermore, based on consensus clustering, the ovarian cancer samples were divided into the C1/ C2 subtype. We found that the Tertiary lymphoid structure (TLS) genes were evidently up-regulated in the C1 subtype than the C2 subtype (figure 2). A previous work has reported the critical roles of TLS in tumor microenvironment and indicates the favorable prognostic outcomes of cancer patients [24]. By using the gene signature of TLS, it provides novel opportunities to predict the immune microenvironment and clinical outcomes of patients with cancer [16]. For instance, Feng *et al.* have reported that the TLS signature high group shows improved survival outcomes and immune infiltration levels in lung adenocarcinoma patients [25]. An et al. have revealed that the TLS genes are related to better prognosis as well as higher immune cells infiltration, and the TLS score constructed by the cox regression and principal component analysis is suggested as the predictor for the TLS pattern and prognosis of bladder cancer patients [26]. In our work, we further analyzed the gene expression pattern in the two molecular subtypes in aOC. Totally 164 up-regulated RNAs and 456 down-regulated RNAs were screened in the subtypes. According to the GO, KEGG as well as the GSEA analysis, these DEGs between ovarian cancer subtypes were linked with the immune response, activation of the immune cells and drug metabolism (figure 3). Compared with the previous studies, our work also revealed that the therapy-induced genomic changes were related to TLS development and immune response in aOC, and the changes in TLS signature genes in different molecular subtypes of aOC patients were identified.

Machine learning has attracted increasing attention in the statistical analysis of cancer diagnosis, prognosis and treatment [27]. In our work, the LASSO-Cox analysis was adopted to develop the prognostic signature in ovarian cancer patients, the coefficients of DEGs were compressed and 31 genes were retained with the optima lambda value = 0.11 and 15 genes were selected based on the multivariate cox analysis, including CFAP161, KLHDC8A, FXYD3, PALMD, USP32P1, ACTN2, TRPC3, COL24A1, AQP11, TMEM167B, SERPINA5, IGLL5, COL6A6, TMIGD3 and AHCYL1 (figure 3), among which several are reported as DEGs in ovarian cancer [28-33].

Substantial literature has revealed that immune cell infiltration status critically affects the prognosis and treatment efficacy in advanced ovarian cancer patients [34-36]. In our work, we identified that C1 subtype showed increased infiltration levels of immune and stromal cells, which was in line with the findings that the C1 subtype was associated with the higher TLS score relative to the C2 subtype. These results indicated that the enhanced anti-tumor responses in the C1 subtype of ovarian cancer patients (figure 4).

In conclusion, this work explored the neoadjuvant chemotherapy and cytoreductive surgery induced genomic changes and immune response in aOC for the first time. Two molecular subtypes of ovarian cancer were identified and the correlation of each subtype with the TLS signature was confirmed. Prognostic signature was constructed based on machine learning and promising prognostic biomarkers were screened. The findings of our work might provide clues for the prediction of treatment response in aOC patients.

ACKNOWLEDGMENT

Not applicable.

Funding: This work was supported by the 2022 Municipal Guiding Science and Technology Plan Project (No. 22217).

Conflicts of interests: The authors declare no conflicts of interest.

Ethical consideration: Not applicable.

Author contribution: L.L. and C.W. conceptualized the study. L.L., W.H., Q.G. are responsible for data collection and analysis. L.L.wrote the original

[DOI: 10.61186/ijrr.22.4.109]

manuscript. C.W. revised the manuscript. All authors read and approved the final manuscript.

REFERENCES

1. Sung H, Ferlay J, Siegel RL, *et al.* (2021) Global cancer statistics 2020: GLOBOCAN estimates of incidence and mortality worldwide for 36 cancers in 185 countries. *CA Cancer J Clin*, ***71(3):*** *209-249.*
2. Ray-Coquard I, Pautier P, Pignata S, *et al.* (2019) Olaparib plus bevacizumab as first-line maintenance in ovarian cancer. *N Engl J Med*, ***381(25):*** *2416-2428.*
3. Gogineni V, Morand S, Staats H, *et al.* (2021) Current ovarian cancer maintenance strategies and promising new developments. *J Cancer*, ***12(1):*** *38-53.*
4. Armstrong DK, Alvarez RD, Bakkum-Gamez JN, *et al.* (2021) Ovarian cancer, version 2.2020, NCCNclinical practice guidelines in oncology. *J Natl Compr Canc Netw*, ***19(2):*** *191-226.*
5. Vergote I, Coens C, Nankivell M, *et al.* (2018) Neoadjuvant chemotherapy versus debulking surgery in advanced tubo-ovarian cancers: pooled analysis of individual patient data from the EORTC 55971 and CHORUS trials. *Lancet Oncol*, ***19(12):*** *1680-1687.*
6. Coleridge SL, Bryant A, Kehoe S, Morrison J (2021) Neoadjuvant chemotherapy before surgery versus surgery followed by chemotherapy for initial treatment in advanced ovarian epithelial cancer. *Cochrane Database Syst Rev*, ***7(7):*** *Cd005343.*
7. Eshaghi M (2020) The effect of pain management on pain reduction in women with breast cancer. *Sjmshm,* ***2(2):*** *1-5.*
8. Merlo LM, Pepper JW, Reid BJ, Maley CC (2006) Cancer as an evolutionary and ecological process. *Nat Rev Cancer*, ***6(12):*** *924-935.*
9. Xiao Y and Yu D (2021) Tumor microenvironment as a therapeutic target in cancer. *Pharmacol Ther*, ***221:*** *107753.*
10. Schumacher TN, Thommen DS (2022) Tertiary lymphoid structures in cancer. *Science*, ***375(6576):*** *eabf9419.*
11. Munoz-Erazo L, Rhodes JL, Marion VC, Kemp RA (2020) Tertiary lymphoid structures in cancer - considerations for patient prognosis. *Cell Mol Immunol*, ***17(6):*** *570-575.*
12. Cottrell TR, Thompson ED, Forde PM, *et al.* (2018) Pathologic features of response to neoadjuvant anti-PD-1 in resected non-small-cell lung carcinoma: a proposal for quantitative immune-related pathologic response criteria (irPRC). *Ann Oncol*, ***29(8):*** *1853-1860.*
13. Vanhersecke L, Brunet M, Guégan JP, *et al.* (2021) Mature tertiary lymphoid structures predict immune checkpoint inhibitor efficacy in solid tumors independently of PD-L1 expression. *Nat Cancer*, ***2 (8):*** *794-802.*
14. Yang M, Lu J, Zhang G, *et al.* (2021) CXCL13 shapes immunoactive tumor microenvironment and enhances the efficacy of PD-1 checkpoint blockade in high-grade serous ovarian cancer. *J Immunother Cancer*, ***9(1)****.*
15. Amini J and Hasanramezani A (2022) AAK1 circular regulates neuronal development by interacting with miR-132, miR-146a and miR484. *Alkhass,* ***4(4):*** *1-4.*
16. Sautès-Fridman C, Petitprez F, Calderaro J, Fridman WH (2019) Tertiary lymphoid structures in the era of cancer immunotherapy. *Nat Rev Cancer*, ***19(6):*** *307-325.*
17. Lu H, Lou H, Wengert G, *et al.* (2023) Tumor and local lymphoid tissue interaction determines prognosis in high-grade serous ovarian cancer. *Cell Rep Med*, ***4(7):*** *101092.*
18. Taminau J, Meganck S, Lazar C, *et al.* (2012) Unlocking the potential of publicly available microarray data using inSilicoDb and inSilicoMerging R/Bioconductor packages. *BMC Bioinformatics*, ***13:*** *335.*
19. Johnson WE, Li C, Rabinovic A (2007) Adjusting batch effects in microarray expression data using empirical Bayes methods. *Biostatistics*, ***8(1):*** *118-127.*
20. McEligot AJ, Poynor V, Sharma R, Panangadan A (2020) Logistic LASSO Regression for Dietary Intakes and Breast Cancer. *Nutrients*, ***12(9)****.*
21. Becht E, Giraldo NA, Lacroix L, *et al.* (2016) Estimating the population abundance of tissue-infiltrating immune and stromal cell populations using gene expression. *Genome Biol*, ***17(1):*** *218.*
22. Elies A, Rivière S, Pouget N, *et al.* (2018) The role of neoadjuvant chemotherapy in ovarian cancer. *Expert Rev Anticancer Ther*, ***18 (6):*** *555-566.*
23. Javellana M, Eckert MA, Heide J, *et al.* (2022) Neoadjuvant chemotherapy induces genomic and transcriptomic changes in ovarian cancer. *Cancer Res*, ***82(1):*** *169-176.*
24. Dieu-Nosjean MC, Giraldo NA, Kaplon H, *et al.* (2016) Tertiary lymphoid structures, drivers of the anti-tumor responses in human cancers. *Immunol Rev*, ***271(1):*** *260-275.*
25. Feng H, Yang F, Qiao L, *et al.* (2021) Prognostic significance of gene signature of tertiary lymphoid structures in patients with lung adenocarcinoma. *Front Oncol*, ***11:*** *693234.*
26. An Y, Sun JX, Xu MY, *et al.* (2022) Tertiary lymphoid structure patterns aid in identification of tumor microenvironment infiltration and selection of therapeutic agents in bladder cancer. *Front Immunol*, ***13:*** *1049884.*
27. Swanson K, Wu E, Zhang A, Alizadeh AA, Zou J (2023) From patterns to patients: Advances in clinical machine learning for cancer diagnosis, prognosis, and treatment. *Cell*, ***186(8):*** *1772-1791.*
28. Zhang L, Wu X, Fan X, Ai H (2023) MUM1L1 as a tumor suppressor and potential biomarker in ovarian cancer: Evidence from bioinformatics analysis and basic experiments. *Comb Chem High Throughput Screen*, ***26(14):*** *2487-2501.*
29. Zhao E, Gao K, Xiong J, *et al.* (2023) The roles of FXYD family members in ovarian cancer: an integrated analysis by mining TCGA and GEO databases and functional validations. *J Cancer Res Clin Oncol.*
30. Zeng B, Yuan C, Yang X, Atkin SL, Xu SZ (2013) TRPC channels and their splice variants are essential for promoting human ovarian cancer cell proliferation and tumorigenesis. *Curr Cancer Drug Targets*, ***13(1):*** *103-116.*
31. Chetry M, Li S, Liu H, Hu X, Zhu X (2018) Prognostic values of aquaporins mRNA expression in human ovarian cancer. *Biosci Rep*, ***38 (2)****.*
32. Bijsmans IT, Smits KM, de Graeff P, *et al.* (2011) Loss of serpinA5 protein expression is associated with advanced-stage serous ovarian tumors. *Mod Pathol*, ***24(3):*** *463-470.*
33. Liang L, Li J, Yu J, *et al.* (2022) Establishment and validation of a novel invasion-related gene signature for predicting the prognosis of ovarian cancer. *Cancer Cell Int*, ***22(1):****118.*
34. Kandalaft LE, Dangaj Laniti D, Coukos G (2022) Immunobiology of high-grade serous ovarian cancer: lessons for clinical translation. *Nat Rev Cancer*, ***22(11):****640-656.*
35. Hornburg M, Desbois M, Lu S, *et al.* (2021) Single-cell dissection of cellular components and interactions shaping the tumor immune phenotypes in ovarian cancer. *Cancer Cell*, ***39(7):*** *928-944.e6.*
36. Li X, Liang W, Zhao H, *et al.* (2021) Immune cell infiltration landscape of ovarian cancer to identify prognosis and immunotherapy-related genes to aid immunotherapy. *Front Cell Dev Biol*, ***9:*** *749157.*

[DOI: 10.61186/ijrr.22.4.109]